Quantum dot bioconjugates for imaging, labelling and sensing

One of the fastest moving and most exciting interfaces of nanotechnology is the use of quantum dots (QDs) in biology. The unique optical properties of QDs make them appealing as *in vivo* and *in vitro* fluorophores in a variety of biological investigations, in which traditional fluorescent labels based on organic molecules fall short of providing long-term stability and simultaneous detection of multiple signals. The ability to make QDs water soluble and target them to specific biomolecules has led to promising applications in cellular labelling, deep-tissue imaging, assay labelling and as efficient fluorescence resonance energy transfer donors. Despite recent progress, much work still needs to be done to achieve reproducible and robust surface functionalization and develop flexible bioconjugation techniques. In this review, we look at current methods for preparing QD bioconjugates as well as presenting an overview of applications. The potential of QDs in biology has just begun to be realized and new avenues will arise as our ability to manipulate these materials improves.

IGOR L. MEDINTZ[1]*, H. TETSUO UYEDA[2], ELLEN R. GOLDMAN[1] AND HEDI MATTOUSSI[2]*

[1]Center for Bio/Molecular Science and Engineering, Code 6900, US Naval Research Laboratory, Washington, DC 20375, USA
[2]Division of Optical Sciences, Code 5611, US Naval Research Laboratory, Washington, DC 20375, USA
*e-mail: Imedintz@cbmse.nrl.navy.mil; Hedimat@ccs.nrl.navy.mil

One of the fundamental goals in biology is to understand the complex spatio–temporal interplay of biomolecules from the cellular to the integrative level. To study these interactions, researchers commonly use fluorescent labelling for both *in vivo* cellular imaging and *in vitro* assay detection[1]. However, the intrinsic photophysical properties of organic and genetically encoded fluorophores, which generally have broad absorption/emission profiles[1] (Fig. 1a) and low photobleaching thresholds, have limited their effectiveness in long-term imaging and 'multiplexing' (simultaneous detection of multiple signals) without complex instrumentation and processing[2]. The seminal publications describing the first biological uses of QD-fluorophores foresaw that their unique properties could overcome these issues[3,4]. QD properties of interest to biologists include high quantum yield, high molar extinction coefficients (~10–100× that of organic dyes)[5,6], broad absorption with narrow, symmetric photoluminescence (PL) spectra (full-width at half-maximum ~25–40 nm) spanning the UV to near-infrared (Fig. 2), large effective Stokes shifts (Fig. 1b,c), high resistance to photobleaching and exceptional resistance to photo- and chemical degradation (Fig. 3a)[7–11]. Compared with molecular dyes, two properties in particular stand out: the unparalleled ability to size-tune fluorescent emission as a function of core size (for binary semiconductor materials), and the broad excitation spectra, which allow excitation of mixed QD populations at a single wavelength far removed (>100 nm) from their respective emissions (Fig. 1b,c). QDs also display intermittency (blinking) under continuous excitation, a property only partially understood, and which has been attributed to Auger ionization[12,13].

SYNTHESIS AND CAPPING STRATEGIES

QDs used in bio-applications are exclusively colloidal nanocrystals. The best available QD fluorophores for biological applications are made of CdSe cores overcoated with a layer of ZnS because this chemistry is the most refined. The ZnS layer passivates the core surface, protects it from oxidation, prevents leeching of the Cd/Se into the surrounding solution and also produces a substantial improvement in the PL yield[5,14]. Even though thin ZnS (1–2 monolayers) shells often

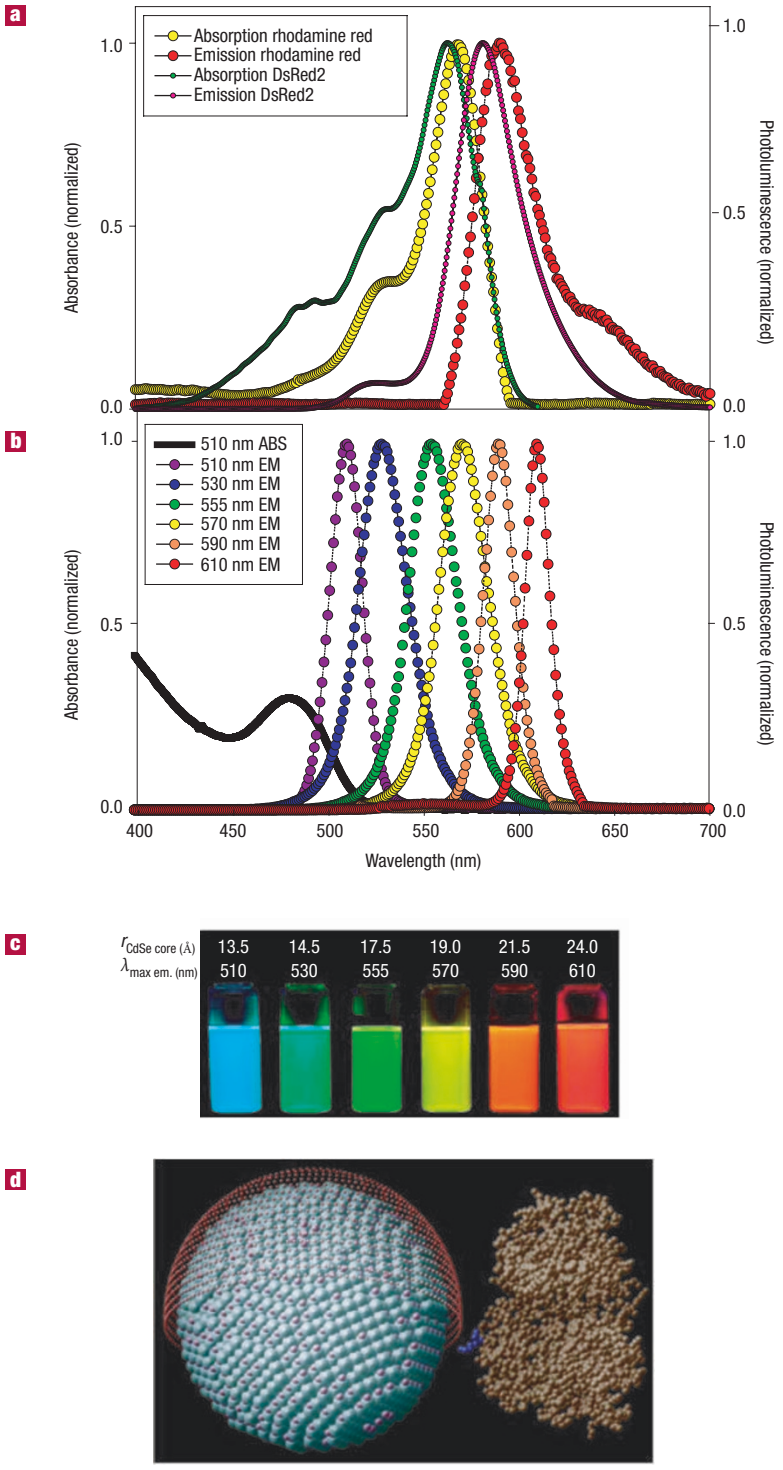

Figure 1 Comparison of rhodamine red/DsRed2 spectral properties to those of QDs highlighting how multiple narrow, symmetric QD emissions can be used in the same spectral window as that of an organic or genetically encoded dye. **a**, Absorption (Abs) and emission (Em) of rhodamine red, a common organic dye and genetically encoded DsRed2 protein[98]. **b**, Absorption and emission of six different QD dispersions. The black line shows the absorption of the 510-nm-emitting QDs. Note that at the wavelength of lowest absorption for the 510-nm QD, ~450 nm, the molar extinction coefficient is greater than that of rhodamine red at its absorption maxima (~150,000 versus 129,000 M^{-1} cm^{-1}). **c**, Photo demonstrating the size-tunable fluorescence properties and spectral range of the six QD dispersions plotted in **b** versus CdSe core size. All samples were excited at 365 nm with a UV source. For the 610-nm-emitting QDs, this translates into a Stokes shift of ~250 nm. *r* = radius **d**, Comparison of QD size to a MBP molecule. 555-nm-emitting CdSe/ZnS core/shell QD, diameter ~60 Å, surface-functionalized with dihydrolipoic acid (red shell ~9–11 Å) has a diameter ~78–82 Å. The diagram depicts the homogeneous orientation MBP assumes relative to the QD (Copyright National Academy of Sciences USA)[53]. MBP a midsize protein (M_r ~ 44 kDa) has dimensions of 30 × 40 × 65 Å (ref. 48).

produce the highest PL yields, thicker ZnS shells (4–6 monolayers) provide more core protection against oxidation and the harsher conditions presented by biological media (for example, acidic buffers and cellular organelles). Colloidal QDs made of ZnS, CdS, ZnSe, CdTe and PbSe, emitting from the UV to the infrared have been prepared[14–29] (Fig. 2); however, these may need refinement for bio-applications as issues of reproducible synthesis and inorganic passivation remain.

The real breakthrough in synthesizing high-quality colloidal QDs came when the Bawendi group reported[24] that use of high-temperature growth solvents/ligands (mixture of trioctyl phosphine/trioctyl phosphine oxide, TOP/TOPO), combined with pyrolysis of organometallic precursors, yielded CdSe QDs with highly crystalline cores and size distributions of 8–11%. The same reaction combined with appropriate organometallic precursors was further used to

overcoat the native CdSe core with a layer of wider-bandgap semiconducting material (for example, ZnS and CdS)[5,14,25]. Fine-tuning this synthetic scheme highlighted the importance of the high-temperature solvent/ligand mixtures, along with using less pyrophoric salt precursors (CdO and Cd-acetate), for preparing reproducible high-quality nanocrystals[15,30].

QDs prepared using high-temperature routes have no intrinsic aqueous solubility, thus phase-transfer to aqueous solution requires surface functionalization with hydrophilic ligands, either through 'cap exchange', a process primarily driven by mass action, or by encapsulating the original nanocrystals in a thick heterofunctional organic coating, driven mainly by hydrophobic absorption onto the TOP/TOPO-capped QDs. These ligands mediate both the colloid's solubility and serve as a point of chemical attachment for biomolecules. Capping ligands serve another critical role in insulating/passivating/protecting the QD surface from deterioration in biological media. Synthesis of new caps create an ever-increasing library available for obtaining aqueous QD dispersions; however, many were created for specialized uses and thus have limited general applicability[3,14,19,26,31–38]. A representative list of caps and the QD-dispersal strategies they use is provided in Table 1. These strategies can be grouped into three major routes. The first uses 'cap exchange' and involves the substitution of the native TOP/TOPO with bifunctional ligands, each presenting a surface-anchoring moiety to bind to the inorganic QD surface (for example, thiol) and an opposing hydrophilic end group (for example, hydroxyl, carboxyl) to achieve water-compatibility. These include an array of thiol and phosphine mono and multidentate ligands (Table 1a,b)[4,26,41–43]. The second strategy involves formation of polymerized silica shells functionalized with polar groups, which insulate the hydrophilic QD (Table 1c)[3,40]. The third method preserves the native TOP/TOPO on the QDs and uses variants of amphiphilic 'diblock' and 'triblock' copolymers and phospholipids to tightly interleave/interdigitate the alkylphosphine ligands through hydrophobic attraction, whereas the hydrophilic outer block permits aqueous dispersion and further derivitization (Table 1d,f,g)[33–36,44–46].

Is there a place for all these different capping strategies? Probably, given that they address the requirements of various potential applications. But the advantages of each strategy have to be carefully weighed against the drawbacks. For example, compact mono-mercapto ligands (Table 1a), although simple to synthesize, have short shelf lives (<1 week) due to dynamic thiol–ZnS interactions[8]. Substitution from mono to dithiol dihydrolipoic acid ligands improves long-term stability from ~1 week to 1–2 years, suggesting that polydentate thiolated ligands could be even more effective[8,26,43]. However, these are carboxylic acids and almost all carboxy-terminated ligands limit dispersion to basic pHs[8]. Silica shells and polymer/phospholipid encapsulation provides stability over a broader pH range, but result in substantially larger hydrophilic QDs. For example, phospholipid and block copolymer coatings tend to increase the diameter of CdSe–ZnS QDs from ~4–8 nm before encapsulation to ~20–30 nm, a size that although smaller than most mammalian cells can still limit intracellular mobility and may preclude

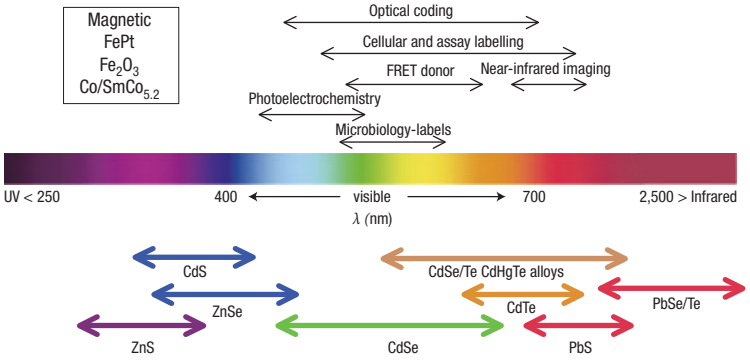

Figure 2 Representative QD core materials scaled as a function of their emission wavelength superimposed over the spectrum. Representative areas of biological interest are also presented corresponding to the pertinent emission highlighting how most biological usage falls in the visible–near infrared region. Inset representative materials used for creating magnetic QDs[14–29,70].

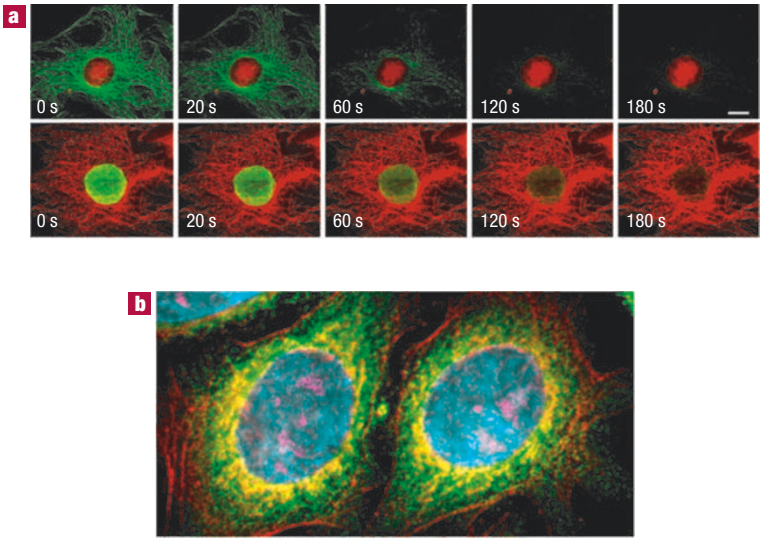

Figure 3 QD resistance to photobleaching and multicolour labelling. **a**, Top row: Nuclear antigens were labelled with QD 630–streptavidin (red), and microtubules were labelled with AlexaFluor 488 (green) simultaneously in a 3T3 cell. Bottom row: Microtubules were labelled with QD 630–streptavidin (red), and nuclear antigens were stained green with Alexa 488. Continuous exposure times in seconds are indicated (Reprinted by permission of the Nature Publishing Group)[34]. Note the QD resistance to photobleaching under continuous illumination. **b**, Pseudocoloured image depicting five-colour QD staining of fixed human epithelial cells. Cyan corresponds to 655-nm Qdots labelling the nucleus, magenta 605-Qdots labelling Ki-67 protein, orange 525-Qdots labelling mitochondria, green 565-Qdots labelling microtubules and red 705-Qdots labelling actin filaments. Courtesy of Quantum Dot Corp.

fluorescence resonance energy transfer (FRET)-based investigations[8]. Lastly, an issue often overlooked in biocompatible QD preparation is monitoring of the ligand-exchange efficiency, because performing effective cap exchange still remains an art form. Clearly needed are systematic analytical techniques evaluating the extent of cap exchange beyond the final functional test[19,46].

INORGANIC–BIOLOGICAL HYBRIDS

Inorganic–biological hybrids are made by conjugating inorganic nanostructures (nanoparticles, nanorods) with biomolecules (proteins, DNAs) and the resulting conjugates combine the properties of both materials, that is, the spectroscopic characteristics of the nanocrystal and the biomolecular function of the surface-attached entities. Owing to its finite size (comparable to or slightly larger than that of many proteins, Fig. 1d) a single QD can be conjugated to several proteins simultaneously. The QD thus acts as a nanoscaffold for attachment of several proteins, or other biomolecules, creating a multifunctional nanoparticle–biological hybrid. Our work has shown that ~15–20 maltose binding proteins (MBP, M_r ~ 44 kDa) can be attached to each 6-nm-diameter QD (Fig. 1d)[48]. In these assemblies, conjugate dimensions depend on key parameters, such as surface cap used and number and size of the biomolecules attached to the surface. The function is dictated by the nature of the biological moieties and their conformation; features that have repercussions on final performance. Proteins that do not have their recognition site exposed away from the QD surface may lose their ability to bind a target.

Conjugation schemes for attaching proteins to QDs can be divided into three categories, each of which has limitations. (i) Use of EDC, 1-ethyl-3-(3-dimethylaminopropyl) carbodiimide, condensation to react carboxy groups on the QD surface to amines; (ii) direct binding to the QD surface using thiolated peptides or polyhistidine (HIS) residues; and (iii) adsorption or non-covalent self-assembly using engineered proteins. Conjugation using EDC condensation applied to QDs capped with thiol-alkyl-COOH ligands often produce intermediate aggregates due to poor QD stability in neutral/acidic buffers. Using this same chemistry for QDs encapsulated with polymeric shells bearing COOH groups produces large conjugates with poor control over the number of biomolecules attached to a single nanocrystal. Moreover, this chemistry is prone to crosslinking and aggregating QDs, because the numerous surface functional sites can bind/crosslink the numerous protein target sites. Nonetheless, this approach was used to prepare commercial QD-streptavidin conjugates having ~20 proteins/conjugate and relatively high quantum yield. Streptavidin-coated QDs are used to attach additional functionalities to the QDs (mostly biotinylated antibodies), however they will bind all biotinylated proteins indiscriminately allowing only one targeted use.

Direct attachment of proteins/peptides to the QD surface is based on two types of QD surface–protein interaction; dative thiol-bonding between QD surface sulphur atoms and cysteine residues[19,49] and metal-affinity coordination of HIS residues to the QD surface Zn atoms (Table 1h)[50,51]. The Weiss group demonstrated the former by using phytochelatin-related peptides to cap CdSe/ZnS core/shell QDs, providing not only surface passivation and water solubility, but also a point of biochemical modification (Table 1h)[19]. Using peptides for both dispersion and biofunctionalization may represent a new class of rationally designed multifunctional biological cap[11,19]. By using metal-affinity coordination, HIS-expressing proteins or peptides can be directly attached to Zn on the QD-surface. This strong interaction (Zn^{2+}-HIS) has a dissociation constant, K_D, only slightly less than that measured for 6-HIS to NTA-Ni^{2+} (10^{-13}) but stronger than most antibody bindings (10^{-6}–10^{-9})[51]. Functional assays with HIS-appended proteins indicate that control can be exerted on the final bioconjugate assembly through the molar ratios of each participant added before self-assembly[48,52–54]. This strategy allows mixed protein surfaces, with the HIS affinity for other metals (Ni, Cu, Co, Fe, Mn) being relevant to future materials[51].

Engineering proteins to express positively charged domains allows them to self-assemble onto the surface of negatively charged QDs through electrostatic assembly[26]. This approach has proved useful for attaching a variety of engineered proteins to QDs including MBP, for purification over amylose resin, and Protein G, which will bind the IgG portion of an antibody thus acting as a linker[55]. Proteins can also be non-specifically adsorbed to QDs[56]. Regardless of the approach used in forming hybrid conjugates, three important issues remain: (i) the aforementioned lack of conjugation strategies; (ii) the lack of homogeneity when attaching proteins to QDs; and (iii) the inability to finely control ratios of proteins/QD. The lack of homogeneous attachment results in heterogeneous protein orientation on the QD surface, which may produce conjugates with surface-attached proteins that are not optimally functional. With antibodies, for example, many may not be correctly oriented to bind their intended target and this will manifest in low avidity. It's worth mentioning that success in bioconjugation is intimately tied into development of new caps, thus QD success in biology will ultimately be driven by cap design.

EXISTING USES OF QUANTUM DOTS IN BIOLOGY

CELLULAR LABELLING

Cellular labelling is where QD use has made the most progress and attracted the greatest interest. Within the last two years, numerous reports have

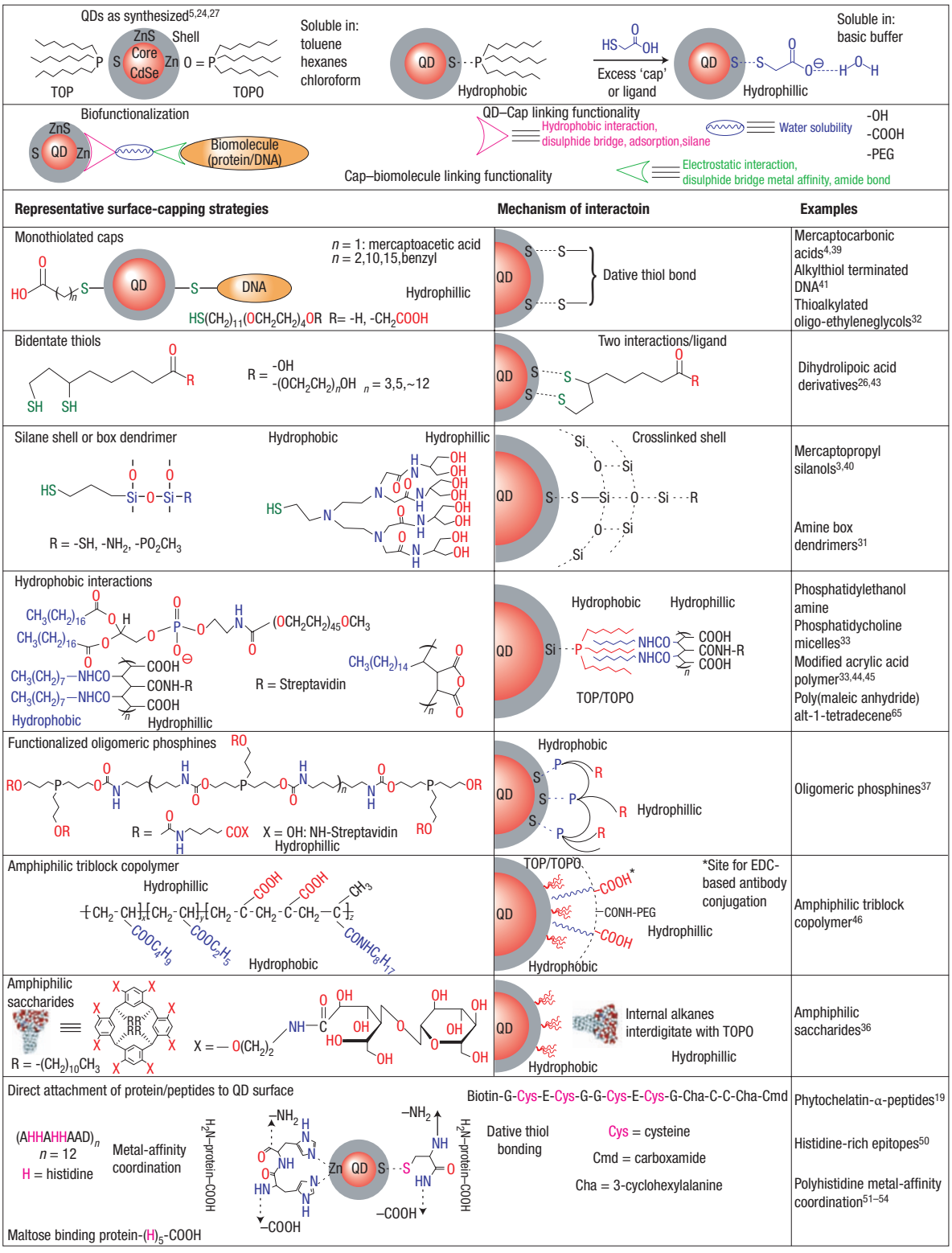

Table 1 Schematic of generic QD solubilization and biofunctionalization (**a–h**). Biofunctionalization (second panel from top) uses caps/ligands to provide three functions. Linkage to the QD (pink), water solubility (blue) and a biomolecule linking functionality (green). Examples of surface-capping strategies and the mechanism of interaction with the QD and the aqueous environment. For the cap exchange (top right) excess thiolated cap displaces the original TOP/TOPO organic coating by binding the ZnS surface with the thiol group and imparting hydrophilicity with the charged carboxyl (or other functionalities) yielding water-soluble colloidal QD dispersions.

Table 2 Representative cellular components and proteins that have been labelled with QDs. *Indicates that labelling was performed in live cells.

Cellular component/protein	Function
Nucleus/nuclear proteins*	Internal organelle containing the genetic information (chromosomal DNA), enclosed by a membrane containing pores that mediate transport in and out[34,61,62]. See Fig. 3.
Mitochondria*	Organelle providing essential energy-delivery processes, contains its own genome[62]. See Fig. 3.
Microtubules	Cytoskeleton protein that maintains cellular structure and reforms during movement[34]. See Fig. 3.
Actin filaments	Cytoskeleton protein that maintains cellular structure, helps localize other organelles and reforms during movement[34]. See Fig. 3.
Endocytic compartments*	Vesicles that form on cell surfaces and mediate both specific and non-specific internalization of extracellular molecules[56,58].
Mortalin	Member of Heat Shock 70 Protein Family. Differential staining pattern in normal and precancerous cells[59].
Cytokeratin	Cytoskeleton protein that is overexpressed and differentially stained in many skin cancer cells[57].
Cellular membrane proteins and receptors	This membrane is a lipid bilayer that encloses the cytoplasm (cellular fluid environment) and contains the membrane spanning channels and receptors that allow the cell to communicate with its environment.
Serotonin transport proteins*	Cell surface transporter of serotonin and related neurotransmitters[69].
Prostate-specific membrane antigen*	Protein expressed on surface of normal and cancerous prostate cells[46].
Her2*	Breast cancer marker protein overexpressed on the surface of some breast cancer cells[34].
Glycine receptors*	Main inhibitory neurotransmitter receptor on surface of spinal nerve cells[66].
erbB/HER*	Cellular membrane spanning receptor that mediates cellular response to growth factors. Once activated, the receptors undergo endocytosis and recycling or degradation. Overexpressed in many cancers[67].
p-glycoprotein*	Multidrug transporter that spans the membrane and is a mediator of multidrug resistance in cancer cells[57,58].

appeared describing the ability of one or more 'colour/size' of biofunctionalized QDs to label cells. Many of these reports show that QD labelling permits extended visualization of cells under continuous illumination as well as multicolour imaging, highlighting the advantages offered by these fluorophores (Table 2, Fig. 3)[34,56–60]. A clear differentiation can be made between labelling of live or 'fixed' cells (dead, with chemically crosslinked components to maintain cellular architecture). Fixed cells can be treated 'harshly' to facilitate entry of the QD reagent by chemically creating pores. For labelling live cells, the process must be handled judiciously to maintain cellular viability. The major hurdle is entry of the relatively large QDs into the cell across the cellular membranes' lipid bilayer. Strategies to accomplish this include non-specific uptake by endocytosis, where QDs often end up in endocytic compartments (Table 2); direct microinjection of nanolitre volumes, which is tedious and limits the number of cells labelled; electroporation, which uses charge to physically deliver QDs through the membrane and mediated/targeted uptake[61–63]. Mediated uptake uses reagents such as Lipofectamine 2000, which encapsulates QDs within lipid vesicles to facilitate entry into the cell[63]. Targeted uptake exploits the cells' propensity to recognize and internalize QDs labelled with specific peptides (for example, HIV-derived TAT peptide) and even deliver them to specific cellular compartments such as the nucleus[61]. Comparison of several of these methods showed that the

mediator Lipofectamine 2000 had the highest delivery efficiency, however, the QDs were delivered in aggregates[62,63]. Others combined techniques by electroporating QDs covered with a nuclear localization sequence into cells and then monitored their translocation into the nuclear compartment[61]. Peptide-targeted uptake looks to be the most specific for delivering dispersed QDs into cells, although it may be limited to cells expressing appropriate receptors. Once delivered inside the cytoplasm of cells, dispersion of the QDs depends strongly on their surface coating and pH stability. QDs capped with COOH-terminated groups often aggregate shortly after introduction, due to their poor stability in acidic conditions, whereas protein-coated QDs are more dispersed in the cytoplasm.

To demonstrate multicolour labelling of live cells, endocytic uptake and selective labelling of cell surface proteins were used with antibody-conjugated QDs, and then QD emission was followed for over a week as cellular development was monitored, showing that cells tolerate QDs for extended periods of time[33,58,65]. By using antibody-linked QDs, both the Her2 breast cancer marker and specific intracellular proteins were labelled in both live and fixed cancer cells, demonstrating that QD-probes can cross into cells and specifically bind their intended intracellular targets[34]. QDs can also be useful markers for tracking cellular movement, differentiation and fate[33,58,65]. Cancer cells seeded on top of QDs engulf them and leave behind a fluorescence-free phagokinetic trail[65]. Using several cell lines, the size and shape of trails were shown to correlate well with potential invasiveness, providing a novel assay for this property[65]. Micelle-stabilized QDs injected into *Xenopus* embryos demonstrated cell lineage-tracing during the complex developmental process spanning the embryo–tadpole stage and equal transfer of QDs from mother to daughter cells, again showing long-term cellular compatibility even with $>10^9$ QDs per cell[33]. By exploiting QD photobleaching resistance, previously onerous cellular physiology questions have been investigated on the single-molecule level. These include tracking the diffusion dynamics of individual glycine receptors in neuronal cells over long periods of time (min), which provided unique information on single-protein movement, and interestingly, the authors used blinking to identify single QDs and differentiate them from aggregates[66]. Additionally, the specific erbB/HER cellular receptor-mediated fusion and internalization process has been observed in single cells[67]. These publications mark the transition from 'proof-of-concept' to useful tool as these complex cellular processes could not be tracked continuously with photolabile organic fluorophores.

IN VIVO AND DEEP TISSUE IMAGING

Imaging tissue with far red/near infrared excitation overcomes some problems due to indigenous tissue autofluorescence, and QD spectroscopic properties can be exploited here to achieve somewhat deeper penetration than the available near-infrared dyes[68–70]. This was demonstrated by synthesizing near-infrared-emitting QDs (840–860 nm) and applying them to sentinel lymph-node mapping in cancer surgery of animals[70]. Using only 5 mW cm^{-2} excitation, they imaged lymph nodes 1 cm deep in tissue, where lymphatic vessels were clearly visualized draining QD solutions into the sentinel nodes (Fig. 4)[70]. As an added bonus, the location of QD accumulation in the excised nodes may be the most likely place for the pathologist to find metastatic cells. Interestingly, QDs have been demonstrated to remain fluorescent in tissues *in vivo* for four months[45]. In addition to the properties described above, QDs have large two-photon cross-sectional efficiency with a two-photon fluorescence process 100–1,000× that of organic dyes. This makes them suitable for *in vivo* deep-tissue imaging using two-photon excitation at low intensities[63,71]. Using this technique to excite green emitting QDs in the near infrared allowed imaging of mice capillaries hundreds of micrometres deep and subcellular resolution of mouse brain[68,71].

QDs may also be useful for tracking cancer cells *in vivo* during metastasis[46,60,63]. A multifunctional QD probe has been developed[46] (Table If) linked with tumour-targeting antibodies. *In vivo* studies in mice expressing human cancer showed that these QD probes accumulated at the tumour sites. Using a slightly different approach, tumour cells were labelled with QDs, injected into mice and then tracked with multiphoton microscopy as they invaded lung tissue[63]. In both studies, spectral imaging and autofluorescent subtraction allowed multicolour *in vivo* visualization of cells and tissues[46,63]. The ability to track cells *in vivo* without continuously sacrificing animals represents a substantial improvement over current techniques.

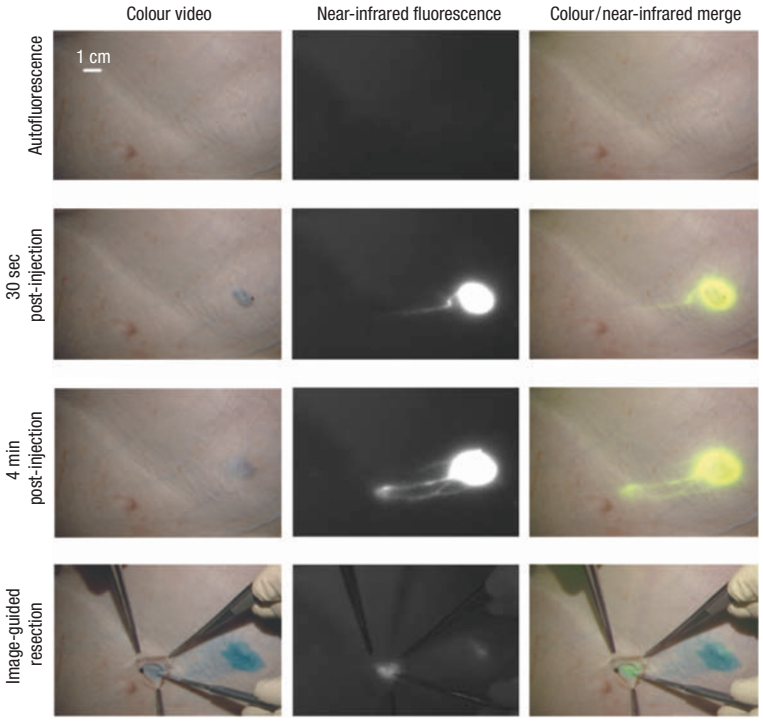

Figure 4 Near-infrared QD imaging *in vivo*. Images of the surgical field in a pig injected intradermally with 400 pmol of near-infrared QDs in the right groin. Four time points are shown from top to bottom: before injection (autofluorescence), 30 s after injection, 4 min after injection and during image-guided resection. For each time point, colour video (left), near-infrared fluorescence (middle) and colour-near infrared merge (right) images are shown. Note the lymphatic vessel draining to the sentinel node from the injection site. (Reprinted by permission of the Nature Publishing Group)[70].

Although QDs are clearly superior to dyes for these purposes, the question of whether the large QD probe mirrors true *in vivo* physiology remains unanswered.

There are many open questions about the toxicity of inorganic QDs containing Cd, Se, Zn, Te, Hg and Pb[72,73]. These can be potent toxins, neurotoxins and teratogens depending on dosage and complexation, accumulating in and damaging the liver and nervous system. In small dosages, the metals are bound by metallothionein proteins and may be excreted slowly or sequestered *in vivo* in adipose and other tissues[64,72]. Although cellular studies have followed QD exposure over time[33,34,58,60,63], to date there have been no long-term animal studies assessing QD toxicology. CdSe QD toxicity has been examined using a hepatocyte culture model and it was found that exposure of core CdSe to an oxidative environment caused decomposition and desorption of Cd ions, whereas adding a shell of 1–2 monolayers of ZnS reduced oxidation, but did not fully eliminate cytotoxicity induced by 8 h of photooxidation[64]. A rather thick ZnS-overcoating (4–6 monolayers) in combination with efficient surface capping/coating can substantially reduce desorption of core ions; nonetheless, extreme radiation can still cause desorption of the core ions[64]. Additionally, it has been reported that QDs could damage DNA[74] and that QD surface coatings effect cytotoxicity[75]. Given the broad interest in QDs, these results are fuelling a strong debate on this issue[64,74,75]. The fact that some long-term *in vivo* studies have not found evidence of toxicity is promising[33,45,58,63], but still not a 'blanket' endorsement. For *in vivo* imaging, if the metals are safely contained, the issue will become one of metabolically clearing the nanoparticle, however, hardly anything is known about how these particles will be cleared by the body[72,73]. Given the myriad materials, preparations and coatings, it is debatable as to whether the definitive comprehensive study will ever be realized.

QD ASSAY LABELLING

QD assay labelling uses QDs for *in vitro* assay detection of DNA, proteins and other biomolecules. DNA-coated QDs have been shown as sensitive and specific DNA labels for *in situ* hybridizations[47], as probes for human metaphase chromosomes[76], and in single-nucleotide polymorphism and multi-allele DNA detection[77]. Conversely, DNA linked to QD surfaces has been used to code and sort the nanocrystals[78]. These results demonstrate that DNA-conjugated QDs specifically bind their complements both in fixed cells and *in vitro*. For proteins, our group uses a self-assembled electrostatic protein QD-functionalization strategy to create QD-based fluoro-immunoassay reagents. Using antibodies conjugated to QDs by an adaptor protein, we have carried out multiple demonstrations of analyte detection in numerous immunoassays including a four-colour multiplex toxin analysis[42,79]. For bioassays, the ability to excite QDs at almost any wavelength below the band edge combined with high photobleaching resistance and 'multiplexing' capabilities highlights the unique combination of spectral properties that make QD-fluorophores of interest to biologist.

QDS AND FRET

As FRET is sensitive to molecular rearrangements on the 1–10 m range (a scale correlating to the size of biological macromolecules), researchers have long used this photophysical process to monitor intracellular interactions and binding events[1]. Reports of QDs as FRET donors in a biological context appeared quickly[39,80,81]; however, the full potential has only been demonstrated recently. By self-assembling acceptor dye-labelled proteins onto QD donor surfaces, two unique advantages over organic fluorophores for FRET became apparent: QD donor emission could be size-tuned to improve spectral overlap with a particular acceptor dye, and having several acceptor dyes interact with a single QD-donor substantially improved FRET efficiency (Fig. 5a,b)[52]. The scenario in Fig. 5b demonstrates the latter using a 30 Å radius QD with a dye-labelled protein attached to the QD surface and the dye located at 70 Å from the core. Assuming a Förster distance (R_0) for this QD donor–dye acceptor pair of 56 Å, then the FRET efficiency for a single donor–acceptor pair would be 22%. By increasing the number of acceptors to five, the efficiency more than doubles to ~58%[48,52].

QDs also function as effective protein nanoscaffolds and exciton donors for prototype self-assembled FRET nanosensors targeting the nutrient maltose by using MBP[48]. QDs could even drive biosensors through a two-step FRET mechanism overcoming inherent donor–acceptor distance limitations, as schematically depicted in Fig. 5c, where each 530-nm QD is surrounded by ~10 MBPs (each mono-labelled with Cy3, one shown for clarity)[48]. β-cyclodextrin-Cy3.5 (β-CD-Cy3.5) specifically bound in the MBP central binding pocket completes the QD-10MBP-Cy3-β-CD-Cy3.5 sensor complex. Excitation of the QD results in FRET excitation of the MBP-Cy3, which in turn FRET-excites the β-CD-Cy3.5 overcoming the low direct QD-Cy3.5 FRET. Added maltose displaces β-CD-Cy3.5 leading to increased Cy3 emission. Using a set of site-specifically dye-labelled MBPs and a FRET strategy analogous to a nanoscale global positioning system determination, the QD-MBP structure was modelled and the results indicate that MBP assumes a homogeneous orientation once assembled on the QD surface (Fig. 1d)[53]. This result suggests that it's possible to self-assemble QD–protein conjugates with the proteins homogeneously oriented; an important finding in light of previous concerns about forming hybrid structures.

Paradoxically, the excellent QD donor properties (long fluorescent lifetime, broad absorption and high extinction coefficient) may almost preclude their role as FRET acceptors for organic dyes[82]. The larger size of 'redder' CdSe and other QDs (emission >600 nm,

Box 1 Developing technologies

Many biological applications of QDs have just begun to be explored. Using combinations of QD emissions to create multicolour optical barcodes is promising, as estimates indicate that with just six colours in 10 different intensities, a library of ~1 million entries could be encoded[89]. However, this remains 'proof-of-concept' with preliminary reports showing that polystyrene beads optically encoded with QDs and targeting DNA can be hybridized and detected at the single bead level[89]. The Willner group have been investigating QD photoelectrochemistry using DNA-driven QD arrays to harness photogenerated currents in the pursuit of novel optoelectronic devices[90]. In an elegant display, CdS QDs were bound in the central pocket of a GroEL chaperonin protein complex, which released this cargo on the addition of ATP (Fig. B1a,b)[91]. GroEL is a cylindrical chaperonin protein complex (M_r ~840 kDa, 4.5 nm cavity) that functions in refolding denatured proteins *in vivo*[91]. The schematic representation shows the formation of GroEL–CdS nanoparticle complexes through inclusion of CdS nanoparticles into the cylindrical cavity of GroEL, and its ATP-triggered guest release along with transmission electron micrographs of these chaperonin–CdS nanoparticle complexes. The models on the sides of the images are schematic representations of the end-view of the complexes (Reprinted by permission of the Nature Publishing Group)[91]. This demonstration bodes well for developing a biosensor or intracellular QD sequestering and delivery mechanism based on controlled QD release in response to a target analyte.

The drive to combine the ability to capture, separate and visualize cells (or proteins) within one reagent is driving interest in biomagnetic QDs. One approach used antibiotic-coated FePt particles to capture and identify bacteria at ultralow concentrations, whereas another used nitriloacetic-acid-coated FePt particles to efficiently capture HIS-appended proteins[17,21]. In an attempt at hybrid magnetic–luminescent QD complexes, polymer-coated Fe_2O_3 cores overcoated with a CdSe-ZnS QD shell and functionalized with antibodies were used to magnetically capture breast cancer cells, which were then viewed fluorescently[92]. A unique bis-functional CdS-FePt luminescent–magnetic dimeric QD particle has been synthesized, however, its biological function remains to be explored[18]. See Fig. B1c for a schematic and high-resolution TEM of the QD-magnetic CdS_FePt nanoparticles. QDs are also promising tools for visualizing *in vitro* protein movements, such as sliding of actin filaments[93,94], as strain-specific microbiological labels[95] and for enzymatic monitoring of DNA replication[96]. QDs have even been tested as contrasting agents for fingerprint dusting[97].

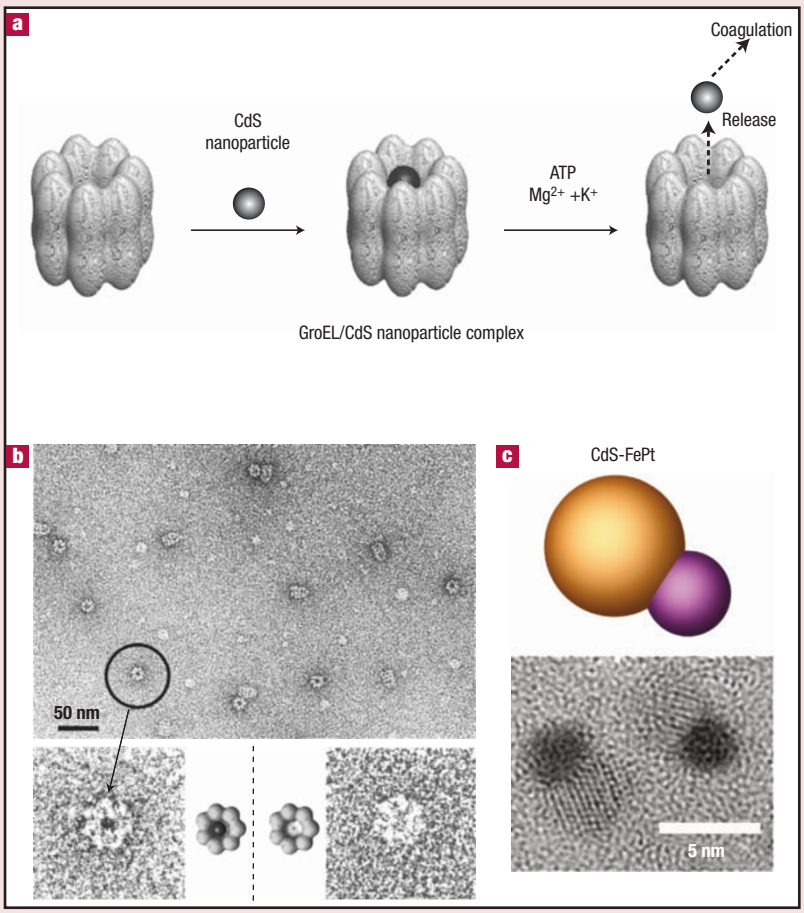

Figure B1 Novel QD bio-applications and materials. **a**, GroEL is a cylindrical chaperonin protein complex (MW ~840 kDa, 4.5 nm cavity) that functions in refolding denatured proteins *in vivo*[91]. Schematic representation of the formation of GroEL–CdS nanoparticle complexes by inclusion of CdS nanoparticles into the cylindrical cavity of GroEL, and its ATP-triggered guest release. **b**, Transmission electron micrographs of chaperonin–CdS nanoparticle complexes. The models on the sides of the images are schematic representations of the end-view of the complexes (Reprinted by permission of the Nature Publishing Group)[91]. **c**, Schematic and high-resolution TEM of QD-magnetic CdS–FePt nanoparticles (Reprinted with permission of the American Chemical Society)[18].

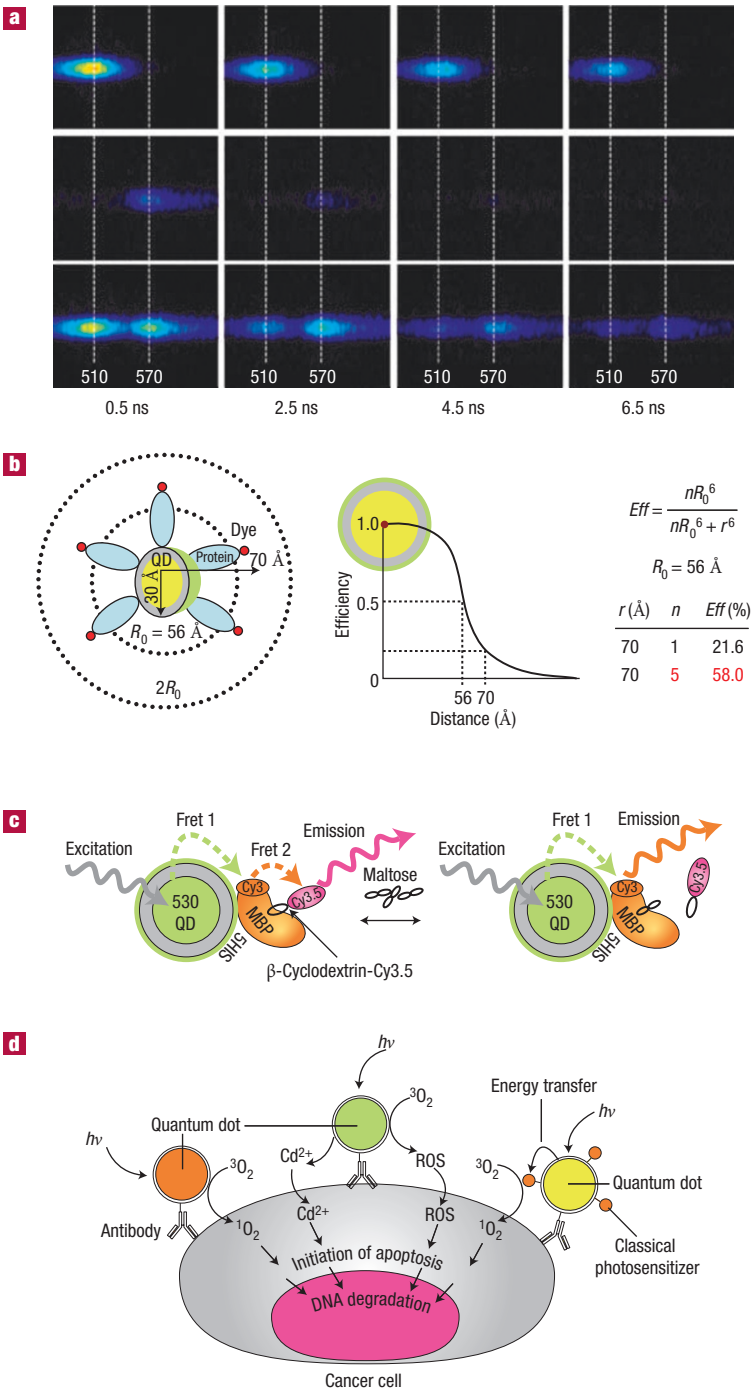

Figure 5 Properties of QDs as FRET donors. **a**, Images displaying FRET between a 510-nm-emitting QD donor and MBP-Cy3 acceptor immediately after a short excitation pulse as recorded by the CCD camera at 2-ns intervals. Panel 1: 510-nm QD donor only, Panel 2: MBP-Cy3 acceptor only, Panel 3: 510-nm QD donor with MBP-Cy3 acceptor self-assembled on the QD surface. (Reprinted by permission of the American Chemical Society)[52]. **b**, Demonstration of improved FRET efficiency (*Eff*) derived from arraying multiple acceptor dyes around a single QD donor acting as a protein scaffold. **c**, Schematic of a 530QD-MBP-Cy3-β-CD-Cy3.5 maltose sensing assembly. (Reprinted by permission of the Nature Publishing Group)[48]. **d**, Schematic of how QD photosensitizers functionalized with cancer cell-specific antibodies would bind and specifically kill a cancer cell *in vivo*. The antibodies direct the QDs to bind only to cancer cells and QDs then harvest either UV or infrared energy (by two-photon excitation) and use this to generate reactive oxygen species, ROS, which initiate apoptosis or programmed cell death (Figure kindly provided by R. Bakalova)[84].

diameter >8 nm) may also preclude FRET as the Förster distance (R_0, donor/acceptor distance for 50% energy transfer) may fall within the core–shell radius, suggesting an upper limit on QD size for FRET[52,53]. Beyond sensors, QD-FRET may have potential medical usage as photosensitizers in photodynamic medical therapy (see Fig. 5d)[83,84].

Other potential QD technologies are outlined in Box 1.

FUTURE OUTLOOK

Cellular labelling will continue to see substantial progress. Studies using 'extensive' multiplexing (6–10 colours) will focus on elucidating complex cellular processes by exploiting QD photobleaching resistance and multicolour resolution. Cellular events will be studied on the single biomolecule level with QDs, although intermittency may become an issue for these types of experiments. Work on near-infrared dots as tissue probes and contrast agents will continue almost exclusively in animal models due to unsettled issues of toxicity, which will remain a hot issue without a definitive near-term answer. Progress in optical bar-coding will encompass some combinatorial chemistry synthesis scheme with the QDs functioning as barcodes for the synthetic products. Application of QD bar-coding to high-throughput or parallel assay formats, such as gene-expression monitoring or drug-discovery assays, can be anticipated. The newly available commercial Qbead and Mosaic Gene Expression technology will stimulate use, however, the cost of the dedicated support equipment needed for decoding may limit broader applications[85]. An interesting derivative of QD-barcodes may include magnetic properties for capture. The bifunctional magnetic/luminescent QDs are intriguing and potentially make an ideal reagent for capturing and visualizing low-copy-number biomolecules. Biofunctionalized paramagnetic nanocrystals targeted to particular *in vivo* sites, such as tumours, may make novel magnetic resonance imaging agents. Using bifunctional QDs for concurrent magnetic resonance imaging and deep-tissue imaging may radically alter *in vivo* imaging[86]. FRET-based QD-biosensors will migrate intracellularly to monitor physiological processes in real-time. Interestingly, the QD multiplexing potential remains almost untapped and so bioassays and studies using more than five colours simultaneously can be expected.

Another intriguing area involves QD 'blinking' or intermittency. Epitaxial QDs do not blink. Recent reports suggest that thiol-reducing agents may suppress colloidal QD blinking even in biological buffers, further suggesting that this process may be modulated[12,13,87]. Understanding of QD blinking processes will slowly be elucidated, and harnessing this phenomenon may create biosensors that truly switch off and on. Use of novel QD rod materials with polarized emission may be of benefit to fluorescence polarization assays[88]. We can also envisage complex QD-bioarrays that incorporate biological functions to be fully integrated into nanodevices for light/energy harvesting, biosensing or molecular electronics.

Will QDs replace fluorescent dyes? No — rather they will complement dye deficiencies in particular applications such as *in vivo* imaging. Moreover, adapting QDs for biological use will teach us critical lessons about creating future inorganic–biological hybrids with direct relevance to many other materials. QDs have far from exhausted their biological potential. The shift to enabling everyday research is now beginning, mostly driven by cellular labelling. Other areas, such as medical imaging, FRET biosensing, assay labelling and optical barcoding are likely to follow suit.

Note added in proof: While this manuscript was in preparation, ref. 99 was published. It provides an excellent overview of QD usage for in vivo imaging and diagnostics.

doi:10.1038/nmat1390

References

1. Miyawaki, A. Visualization of the spatial and temporal dynamics of intracellular signaling. *Dev. Cell* **4,** 295–305 (2003).
2. Schrock, E. *et al.* Multicolor spectral karyotyping of human chromosomes. *Science* **273,** 494–497 (1996).
3. Bruchez, M., Jr, Moronne, M., Gin, P., Weiss, S. & Alivisatos, A. P. Semiconductor nanocrystals as fluorescent biological labels. *Science* **281,** 2013–2016 (1998).
4. Chan, W. C. W. & Nie, S. Quantum dot bioconjugates for ultrasensitive nonisotopic detection. *Science* **281,** 2016–2018 (1998).
5. Dabbousi, B. O. *et al.* (CdSe)ZnS core-shell quantum dots: synthesis and optical and structural characterization of a size series of highly luminescent materials. *J. Phys. Chem. B* **101,** 9463–9475 (1997).
6. Leatherdale, C. A., Woo, W. K., Mikulec, F. V. & Bawendi, M. G. On the absorption cross section of CdSe nanocrystal quantum dots. *J. Phys. Chem. B* **106,** 7619–7622 (2002).
7. Murphy, C. J. Optical sensing with quantum dots. *Anal. Chem.* **74,** 520A–526A (2002).
8. Parak, W. J. *et al.* Biological applications of colloidal nanocrystals. *Nanotech.* **14**, R15–R27 (2003).
9. Niemeyer, C. M. Nanoparticles, proteins, and nucleic acids: biotechnology meets materials science. *Angew. Chem. Int. Edn Eng.* **40,** 4128–4158 (2001).
10. Alivisatos, P. The use of nanocrystals in biological detection. *Nature Biotechnol.* **22,** 47–52 (2004).
11. Mattoussi, H., Kuno, M. K., Goldman, E. R., Anderson, G. P. & Mauro, J. M. in *Optical Biosensors: Present and Future* (eds Ligler, F. S. & Rowe C. A.) 537–569 (Elsevier, Amsterdam, Netherlands, 2002).
12. Nirmal, M. *et al.* Fluorescence intermittency in single cadmium selenide nanocrystals. *Nature* **383,** 802–806 (1996).
13. Efros, A. L. & Rosen, M. Random telegraph signal in the photoluminescence intensity of a single quantum dot. *Phys. Rev. Lett.* **78,** 1110–1113 (1996).
14. Hines, M. A. & Guyot-Sionnest, P. Synthesis and characterization of strongly luminescing ZnS-Capped CdSe nanocrystals. *J. Phys. Chem.* **100,** 468–471 (1996).
15. Peng, Z. A. & Peng, X. Formation of high-quality CdTe, CdSe, and CdS nanocrystals using CdO as precursor. *J. Am. Chem. Soc.* **123,** 183–184 (2001).
16. Bailey, R. E. & Nie, S. Alloyed semiconductor quantum dots: tuning the optical properties without changing the particle size. *J. Am. Chem. Soc.* **125,** 7100–7106 (2003).
17. Gu, H., Ho, P.-L., Tsang, K. W. T., Wang, L. & Xu, B. Using Biofunctional magnetic nanoparticles to capture vancomycin-resistant enterococci and other gram-positive bacteria at ultralow concentration. *J. Am. Chem. Soc.* **125,** 15702–15703 (2003).
18. Gu, H., Zheng, R., Zhang, X. & Xu, B. Facile one-pot synthesis of bifunctional heterodimers of nanoparticles: A conjugate of quantum dot and magnetic nanoparticles. *J. Am. Chem. Soc.* **126,** 5664–5665 (2004).
19. Pinaud, F., King, D., Moore, H.-P. & Weiss, S. Bioactivation and cell targeting of semiconductor CdSe/ZnS nanocrystals with phytochelatin-related peptides. *J. Am. Chem. Soc.* **126,** 6115–6123 (2004).
20. Tsay, J. M., Pflughoefft, M., Bentolila, L. A. & Weiss, S. Hybrid approach to the synthesis of highly luminescent CdTe/ZnS and CdHgTe/ZnS nanocrystals. *J. Am. Chem. Soc.* **126,** 1926–1927 (2004).
21. Xu, C. J. *et al.* Nitrilotriacetic acid-modified magnetic nanoparticles as a general agent to bind histidine-tagged proteins. *J. Am. Chem. Soc.* **126,** 3392–3393 (2004).
22. Murray, C. B., Kagan, C. R. & Bawendi, M. G. Synthesis and characterization of monodisperse nanocrystals and close-packed nanocrystal assemblies. *Ann. Rev. Mater. Sci.* **30,** 545–610 (2000).
23. Xu, C. J. *et al.* Dopamine as a robust anchor to immobilize functional molecules on the iron oxide shell of magnetic nanoparticles. *J. Am. Chem. Soc.* **126,** 5664–5665 (2004).
24. Murray, C. B., Norris, D. J. & Bawendi, M. G. Synthesis and characterization of nearly monodisperse CdE (E = sulfur, selenium, tellurium) semiconductor nanocrystallites. *J. Am. Chem. Soc.* **115,** 8706–8715 (1993).
25. Peng, X., Schlamp, M. C., Kadavanich, A. V. & Alivisatos, A. P. Epitaxial growth of highly luminescent CdSe/CdS core/shell nanocrystals with photostability and electronic accessibility. *J. Am. Chem. Soc.* **119,** 7019–7029 (1997).
26. Mattoussi, H. *et al.* Self-assembly of CdSe-ZnS quantum dot bioconjugates using an engineered recombinant protein. *J. Am. Chem. Soc.* **122,** 12142–12150 (2000).
27. Hines, M. A. & Guyot-Sionnest, P. Bright UV-blue luminescent colloidal ZnSe nanocrystals. *J. Phys. Chem. B* **102,** 3655–3657 (1998).
28. Suyver, J. F., Wuister, S. F., Kelly, J. J. & Meijerink, A. Synthesis and photoluminescence nanocrystalline ZnS:Mn^{2+}. *Nano Lett.* **1,** 429–433 (2001).
29. Artmeyev, M. V., Gaponenko, S. V., Germanenko, I. N. & Kapitonov, A. M. Irreversible photochemical spectral hole burning in quantum-sized CdS nanocrystals embedded in a polymeric film. *Chem. Phys. Lett.* **243,** 450–455 (1995).
30. Reiss, P., Bleuse, J. & Pron, A. Highly luminescent CdSe/ZnSe core/shell nanocrystals of low size dispersion. *Nano Lett.* **2,** 781–784 (2002).
31. Guo, W., Li, J. J., Wang, Y. A. & Peng, X. Conjugation chemistry and bioapplications of semiconductor box nanocrystals prepared via dendrimer bridging. *Chem. Mater.* **15,** 3125–3133 (2003).
32. Hong, R. *et al.* Control of protein structure and function through surface recognition by tailored nanoparticle scaffolds. *J. Am. Chem. Soc.* **126,** 739–743 (2004).
33. Dubertret, B. *et al.* In vivo imaging of quantum dots encapsulated in phospholipids micelles. *Science* **298,** 1759–1762 (2002).
34. Wu, X. *et al.* Immunofluorescent labeling of cancer marker Her2 and other cellular targets with semiconductor quantum dots. *Nature Biotechnol.* **21,** 41–46 (2003).
35. Pellegrino, T. *et al.* Hydrophobic nanocrystals coated with an amphiphilic polymer shell: A general route to water soluble nanocrystals. *Nano Lett.* **4,** 703–707 (2004).
36. Osaki, F., Kanamori, T., Sando, S., Sera, T. & Aoyama, Y. A quantum dot conjugated sugar ball and its cellular uptake on the size effects of endocytosis in the subviral region. *J. Am. Chem. Soc.* **126,** 6520–6521 (2004).
37. Kim, S. & Bawendi, M. G. Oligomeric ligands for luminescent and stable nanocrystal quantum dots. *J. Am. Chem. Soc.* **125,** 14652–14653 (2003).
38. Wang, X.-S. *et al.* Surface passivation of luminescent colloidal quantum dots with poly(dimethylaminoethyl methacrylate) through a ligand exchange process. *J. Am. Chem. Soc.* **126,** 7784–7785 (2004).
39. Willard, D. M., Carillo, L. L., Jung, J. & Van Orden, A. CdSe-ZnS quantum dots as resonance energy transfer donors in a model protein-protein binding assay. *Nano Lett.* **1,** 469–474 (2001).
40. Gerion, D. *et al.* Synthesis and properties of biocompatible water-soluble silicacoated CdSe/ZnS semiconductor quantum dots. *J. Phys. Chem. B* **105,** 8861–8871 (2001).
41. Mitchell, G. P., Mirkin, C. A. & Letsinger, R. L. Programmed assembly of DNA functionalized quantum dots. *J. Am. Chem. Soc.* **121,** 8122–8123 (1999).
42. Goldman, E. R. *et al.* Avidin: a natural bridge for quantum dot-antibody conjugates. *J. Am. Chem. Soc.* **124,** 6378–6382 (2002).
43. Uyeda, H. T., Medintz, I, L., Jaiswal, J. K., Simon, S. M. & Mattoussi H. Synthesis of compact multidentate ligands to prepare stable hydrophilic quantum dot fluorophores. *J. Am. Chem. Soc.* **127**,3870–3878 (2005).
44. Mattheakis, L. C. *et al.* Optical coding of mammalian cells using semiconductor quantum dots. *Anal. Biochem.* **327,** 200–208 (2004).
45. Ballou, B., Lagerholm, B. C., Ernst, L. A., Bruchez, M. P. & Waggoner, A. S. Noninvasive imaging of quantum dots in mice. *Bioconj. Chem.* **15,** 79–86 (2004).
46. Gao, X., Cui, Y., Levenson, R. M., Chung, L. W. K. & Nie, S. In vivo cancer targeting and imaging with semiconductor quantum dots. *Nature Biotechnol.* **22,** 969–976 (2004).
47. Pathak, S., Choi, S. K., Arnheim, N. & Thompson, M. E. Hydroxylated quantum dots as luminescent probes for in situ hybridization. *J. Am. Chem. Soc.* **123,** 4103–4104 (2001).
48. Medintz, I. L. *et al.* Self-assembled nanoscale biosensors based on quantum dot FRET donors. *Nature Mater.* **2,** 630–638 (2003).
49. Akerman, M. E., Chan, W. C. W., Laakkonen, P., Bhatia, S. N. & Ruoslahti, E. Nanocrystal targeting in vivo. *Proc. Natl Acad. Sci.* **99,** 12617–12621 (2002).
50. Slocik, J. M., Moore, J. T. & Wright, D. W. Monoclonal antibody recognition of histidine-rich peptide encapsulated nanoclusters. *Nano Lett.* **2,** 169–173 (2002).
51. Hainfeld, J. F., Liu, W., Halsey, C., M. R., Freimuth, P. & Powell, R., D. Ni-NTAgold clusters target His-tagged proteins. *J. Stuct. Biol.* **127,** 185–198 (1999).
52. Clapp, A. R. *et al.* Fluorescence resonance energy transfer between quantum dot donors and dye-labeled protein acceptors. *J. Am. Chem. Soc.* **126,** 301–310 (2004).
53. Medintz, I., L. *et al.* A fluorescence resonance energy transfer derived structure of a quantum dot-protein bioconjugate nanoassembly. *Proc. Natl Acad. Sci.* **101,** 9612–9617 (2004).
54. Medintz, I. L., Trammell, S. A., Mattoussi, H. & Mauro, J. M. Reversible modulation of quantum dot photoluminescence using a protein-bound photochromic fluorescence resonance energy transfer acceptor. *J. Am. Chem. Soc.* **126,** 30–31 (2004).

55. Goldman, E. R. *et al.* Conjugation of luminescent quantum dots with antibodies using an engineered adaptor protein to provide new reagents for fluoroimmunoassays. *Anal. Chem.* **74,** 841–847 (2002).
56. Hanaki, K. *et al.* Semiconductor quantum dot/albumin complex is a long-life and highly photostable endosome marker. *Biochem. Biophys. Res. Comm.* **302,** 496–501 (2003).
57. Sukhanova, A. *et al.* Biocompatible fluorescent nanocrystals for immunolabeling of membrane proteins and cells. *Anal. Biochem.* **324,** 60–67 (2004).
58. Jaiswal, J. K., Mattoussi, H., Mauro, J. M. & Simon, S. M. Long-term multiple color imaging of live cells using quantum dot bioconjugates. *Nature Biotechnol.* **21,** 47–51 (2003).
59. Kaul, Z. *et al.* Mortalin imaging in normal and cancer cells with quantum dot immuno-conjugates. *Cell Res.* **13,** 503–507 (2003).
60. Hoshino, A., Hanaki, K.-I., Suzuki, K. & Yamamoto, K. Applications of T lymphoma labeled with fluorescent quantum dots to cell tracing markers in mouse body. *Biochem. Biophys. Res. Comm.* **314,** 46–53 (2004).
61. Chen, F. & Gerion, D. Fluorescent CdSe/ZnS nanocrystal-peptide conjugates for long-term, nontoxic imaging and nuclear targeting in living cells. *Nano Lett.* **4,** 1827–1832 (2004).
62. Derfus, A. M., Chan, W. C. W. & Bhatia, S. N. Intracellular delivery of quantum dots for live cell labeling and organelle tracking. *Adv. Mater.* **16,** 961–966 (2004).
63. Voura, E. B., Jaiswal, J. K., Mattoussi, H. & Simon, S. M. Tracking early metastatic progression with quantum dots and emission scanning microscopy. *Nature Med.* **10,** 993–998 (2004).
64. Derfus, A. M., Chan, W. C. W. & Bhatia, S. N. Probing the cytotoxicity of semiconductor quantum dots. *Nano Lett.* **4,** 11–18 (2004).
65. Pellegrino, T. *et al.* Quantum dot-based cell motility assay. *Differentiation* **71,** 542–548 (2003).
66. Dahan, M. *et al.* Diffusion dynamics of glycine receptors revealed by singlequantum dot tracking. *Science* **302,** 442–445 (2003).
67. Lidke, D. S. *et al.* Quantum dot ligands provide new insights into erbB/HER receptor-mediated signal transduction. *Nature Biotechnol.* **22,** 198–203 (2004).
68. Levene, M. J., Dombeck, D. A., Kasischke, K. A., Molloy, R. P. & Webb, W. W. In vivo multiphoton microscopy of deep brain tissue. *J. Neurophys.* **91,** 1908–1912 (2004).
69. Rosenthal, S. J. *et al.* Targeting cell surface receptors with ligand-conjugated nanocrystals. *J. Am. Chem. Soc.* **124,** 4586–4594 (2002).
70. Kim, S. *et al.* Near-infrared fluorescent type II quantum dots for sentinel lymph node mapping. *Nature Biotechnol.* **22,** 93–97 (2004).
71. Larson, D. R. *et al.* Water-soluble quantum dots for multiphoton fluorescence imaging in vivo. *Science* **300,** 1434–1437 (2003).
72. Colvin, V. L. The potential environmental impact of engineered nanomaterials. *Nature Biotechnol.* **21,** 1166–1170 (2003).
73. Hoet, P. H., Bruske-Hohlfeld, I. & Salata, O. V. Nanoparticles - known and unknown health risks. *J. Nanobiotechnol.* **2,** 2–12 (2004).
74. Green, M. & Howman, E. Semiconductor quantum dots and free radical induced DNA nicking. *Chem. Comm.* 121–123 (2005).
75. Kirchner, C. *et al.* Cytotoxicity of colloidal CdSe and CdSe/ZnS nanoparticles. *Nano Lett.* **5,** 331–338 (2005).
76. Xiao, Y. & Barker, P. E. Semiconductor nanocrystal probes for human metaphase chromosomes. *Nucl. Acids Res.* **32,** 3 e28 (2004).
77. Gerion, D. *et al.* Room-temperature single-nucleotide polymorphism and multiallele DNA detection using fluorescent nanocrystals and microarrays. *Anal. Chem.* **75,** 4766–4772 (2003).
78. Gerion, D. *et al.* Sorting fluorescent nanocrystals with DNA. *J. Am. Chem. Soc.* **124,** 7070–7074 (2002).
79. Goldman, E. R. *et al.* Multiplexed toxin analysis using four colors of quantum dot fluororeagents. *Anal. Chem.* **76,** 684–688 (2004).
80. Mamedova, N. N., Kotov, N. A., Rogach, A. L. & Studer, J. Albumin-CdTe nanoparticle bioconjugates: preparation, structure, and interunit energy transfer with antenna effect. *Nano Lett.* **1,** 281–286 (2001).
81. Tran, P. T., Goldman, E. R., Anderson, G. P., Mauro, J. M., & Mattoussi, H. Use of luminescent CdSe-ZnS nanocrystal bioconjugates in quantum dot-based nanosensors. *Phys. Status Solidi B* **229,** 427–432 (2002).
82. Clapp, A. R., Medintz, I. L., Fisher, B. R., Anderson, G. P. & Mattoussi, H. Can luminescent quantum dots be efficient energy acceptors with organic dye donors. *J. Am. Chem. Soc.* **127,** 1242–1250 (2005).
83. Samia, A. C. S., Chen, X. & Burda, C. Semiconductor quantum dots for photodynamic therapy. *J. Am. Chem. Soc.* **125,** 15736–15737 (2003).
84. Bakalova, R., Ohba, H., Zhelev, Z., Ishikawa, M. & Baba, Y. Quantum dots as photosensitizers. *Nature Biotechnol.* **22,** 1360–1361 (2004).
85. Xu, H. X. *et al.* Multiplexed SNP genotyping using the Qbead (TM) system: a quantum dot-encoded microsphere-based assay. *Nucl. Acids Res.* **31,** 8 e43 (2003).
86. Josephson, L., Kircher, M. F., Mahmood, U., Tang, Y. & Weissleder, R. Nearinfrared fluorescent nanoparticles as combined MR/optical imaging probes. *Bioconj. Chem.* **13,** 554–560 (2002).
87. Hohng, S. & Ha, T. Near-complete suppression of quantum dot blinking in ambient conditions. *J. Am. Chem. Soc.* **126,** 1324–1325 (2004).
88. Hu, J. *et al.* Linearly polarized emission from colloidal semiconductor quantum rods. *Science* **292,** 2060–2063 (2001).
89. Han, M., Gao, X., Su, J. Z. & Nie, S. Quantum-dot-tagged microbeads for multiplexed optical coding of biomolecules. *Nature Biotechnol.* **19,** 631–635 (2001).
90. Katz, E. & Willner, I. Integrated nanoparticle-biomolecule hybrid systems: synthesis, properties, applications. *Angew. Chem. Int. Edn Eng.* **43,** 6042–6108 (2004).
91. Ishii, D. *et al.* Chaperonin-mediated stabilization and ATP-triggered release of semiconductor nanoparticles. *Nature* **423,** 628–632 (2003).
92. Wang, D., He, J., Rosenzweig, N. & Rosenzweig, Z. Superparamagnetic Fe2O3 beads-CdSe/ZnS quantum dots core-shell nanocomposite particles for cell separation. *Nano Lett.* **4,** 409–413 (2004).
93. Mansson, A. *et al.* In vitro sliding of actin filaments labelled with single quantum dots. *Biochem. Biophys. Res. Comm.* **314,** 529–534 (2004).
94. Bachand, G. D. *et al.* Assembly and transport of nanocrystal CdSe quantum dot nanocomposites using microtubules and kinesin motor proteins. *Nano Lett.* **4,** 817–821 (2004).
95. Kloepfer, J. A. *et al.* Quantum dots as strain- and metabolism-specific microbiological labels. *App. Environ. Microbiol.* **69,** 4205–4213 (2003).
96. Patolsky, F. *et al.* Lighting-up the dynamics of telomerization and DNA replication by CdSe-ZnS quantum dots. *J. Am. Chem. Soc.* **125,** 13918–13919 (2003).
97. Menzel, E. R. *et al.* Photoluminescent semiconductor nanocrystals for fingerprint detection. *J. Forens. Sci.* **45,** 545–551 (2000).
98. Baird, G. S., Zacharias, D. A. & Tsien, R. Y. Biochemistry, mutagenesis, and oligomerization of DsRed, a red fluorescent protein from coral. *Proc. Natl Acad. Sci.* **97,** 11984–11989 (2000).
99. Michalet, X. *et al.* Quantum dots for live cells, in vivo imaging, and diagnostics. *Science* **307,** 538–544 (2005).

Acknowledgements

The authors acknowledge the Naval Research Laboratory (NRL) and A. Ervin and L. Chrisey at the Office of Naval Research (ONR grant N001404WX20270) and A. Krishan at DARPA for support. I.L.M. was and H.T.U. is supported by a National Research Council Fellowship through NRL.
Correspondence should be addressed to I.M. or H.M.

Competing interests statement

The authors declare that they have no competing financial interests.